Magnetic force microscopy in the presence of a strong probe field

Inhee Lee, Jongjoo Kim, Yuri Obukhov, Palash Banerjee, Gang Xiang, Denis V. Pelekhov, Adam Hauser, Fengyuan Yang, and P. Chris Hammel

Citation: Applied Physics Letters **99**, 162514 (2011); doi: 10.1063/1.3653281
View online: http://dx.doi.org/10.1063/1.3653281
View Table of Contents: http://scitation.aip.org/content/aip/journal/apl/99/16?ver=pdfcov
Published by the AIP Publishing

Magnetic force microscopy in the presence of a strong probe field

Inhee Lee,[a] Jongjoo Kim, Yuri Obukhov, Palash Banerjee, Gang Xiang, Denis V. Pelekhov, Adam Hauser, Fengyuan Yang, and P. Chris Hammel[b]
Department of Physics, The Ohio State University, Columbus, Ohio 43210, USA

(Received 30 August 2011; accepted 27 September 2011; published online 21 October 2011)

We describe a magnetic force microscopy (MFM) imaging approach in which we take advantage of the strong, localized magnetic field of the MFM probe to deterministically modify the magnetization of the sample. This technique enables quantitative mapping of sample magnetic properties including saturation magnetization and anisotropy, a capability not generally available using conventional MFM methods. This approach yields a fruitful theoretical analysis that accurately describes representative experimental data we obtain from an isolated permalloy disk. © *2011 American Institute of Physics*. [doi:10.1063/1.3653281]

Magnetic force microscopy (MFM) is a powerful and widely used technique for studying magnetic micro- and nano-structures.[1–5] MFM provides a 2D spatial map of the gradient of the stray magnetic field emanating from inhomogeneities and discontinuities in ferromagnetic samples such as magnetic domains, vortices, and sample edges. These maps, with typical lateral resolution as good as ~10 nm, usually provide only *qualitative* information about a sample. However, there has been much recent progress developing MFM techniques that provide *quantitative* magnetic information.[6–9] These approaches employ knowledge of the magnetic structure of the scanned probe to deduce the sample magnetization distribution from the experimentally recorded spatial MFM force map. The success of such approaches is limited by the accuracy of their knowledge of the MFM probe.[10–12]

Typically MFM images are obtained in the so-called "hard" magnetic regime in which the strength of the magnetic probe-sample interaction is sufficiently weak that it affects neither the magnetic structure of the sample nor the magnetic probe. This is typically achieved by using low magnetic moment MFM probes whose weak stray magnetic field minimally disturbs the sample. This is important for the study of magnetically unstable structures such as domains and vortices. The theoretical analysis of this hard magnetic case is somewhat simpler[6] than that of an experiment in the "soft" regime where the probe or the sample is affected by the mutual magnetic interaction. This soft regime has been employed for the creation or modification of the magnetic structure of a sample,[13–16] tip characterization,[17] and magnetic sample imaging.[18] However, quantitative analysis of data acquired in either regime is made difficult by incomplete knowledge of the magnetic configuration of the sample and magnetic probe.

Here, we describe an approach to quantitative MFM imaging that employs a strong external magnetic field to define the magnetic configuration of both the sample and the MFM probe. In our approach, the local perturbation of sample magnetization introduced by the stray magnetic field of a high coercivity MFM probe is used to extract and spatially map materials parameters such as saturation magnetization and anisotropy from extended magnetic samples. Our approach employs a strong magnetic field $\mathbf{H}_0$ applied along the $\hat{z}$ axis which saturates the sample in conjunction with the strong magnetic field $\mathbf{H}^p$ of a high magnetization MFM probe magnet. In our case, the micromagnetic probe consists of a Sm_2Co_{17} particle glued to a commercial Si cantilever and micromachined using a focused ion beam into a ~1 μm cube with magnetic moment $m \sim 10^{-9}$ emu and coercive field $H_c \sim 17$ kG, both determined using cantilever magnetometry.[19,20] Of course, a uniformly magnetized sample will exert no force on an MFM probe,[2] but the strong non-uniform magnetic field of our probe magnet, which can be as high as several kG, locally alters the sample magnetization as shown schematically in Fig. 1(b). This local magnetic inhomogeneity generates a measurable MFM signal force. Because the orientation of the sample magnetization in the vicinity of the probe is defined by the known fields $\mathbf{H}^p$ and $\mathbf{H}_0$, the magnitude of this force can be accurately determined and used to extract quantitative magnetic information from MFM images.

The force $\mathbf{F}$ between the probe magnet, approximated by a point dipole with a moment m_p, and a thin film of thickness t (see Fig. 1) can be expressed as a surface integral

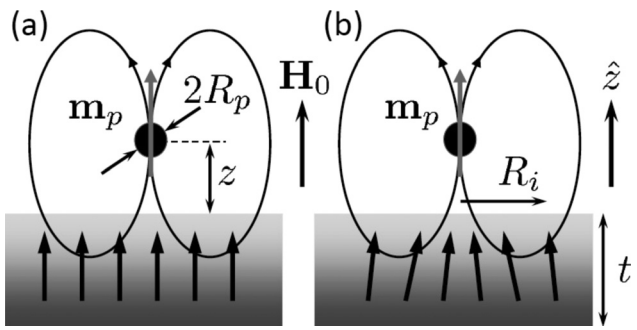

FIG. 1. Geometry of the experiment. A spherical MFM probe of effective radius R_p and magnetic moment m_p is positioned at distance z (measured from the center of the probe) from the surface of a magnetic film of thickness t in a magnetic field H_0 applied perpendicular to the film. The effective radius of the probe-sample interaction R_i is shown schematically. In addition, two sample magnetization profiles are shown schematically: (a) the "hard" magnetic case with sample magnetization unaffected by the probe and (b) where film is magnetized by the strong inhomogeneous probe field.

[a]Electronic mail: ilee@bnl.gov.
[b]Electronic mail: hammel@physics.osu.edu.

$$\mathbf{F} = t\int_S (\mathbf{M}\cdot\nabla)\mathbf{H}^p dS,$$

where $\mathbf{M}$ is the spatially dependent magnetization of the film. The quantity measured in an MFM experiment, the $\hat{z}$ component of this force, is given by

$$F_z = t\int_S \left(M_\perp \frac{\partial}{\partial z}H^p_\perp + M_{||}\frac{\partial}{\partial z}H^p_{||}\right)dS,$$

where $\perp$ and $||$ denote the components of a vector orthogonal and parallel to the film surface, respectively. The orientation of the film magnetization is given by the direction of the total internal field in the film $\mathbf{H}^t$, which includes the applied $\mathbf{H}_0$, demagnetizing $\mathbf{H}^d$, probe $\mathbf{H}^p$, anisotropy $\mathbf{H}^a$, and exchange $\mathbf{H}^{ex}$ fields, and is assumed not to vary across the film thickness. We can then write $M_\perp = M_s \cdot H^t_\perp/H^t$ and $M_{||} = M_s \cdot H^t_{||}/H^t$, where M_s is the local saturation magnetization of the film.

If a thin magnetic film is saturated in a sufficiently strong external out-of-plane magnetic field H_0 in the presence of a probe MFM magnet, then it can be shown that $H^t_\perp \approx H_0 - 4\pi M_s + H^p_\perp + H^a_\perp$ while $H^t_{||} \approx H^p_{||}$. Here, we disregard $H^d_{||}$ for a thin film, $H^a_{||}(\ll H^p_{||})$ for simplicity, and H^{ex} for probe-sample separations greater than 100 nm. Moreover, H_0 can be always adjusted so that $H^t_\perp \gg H^t_{||}$ resulting in $H^t_\perp/H^t \approx 1$; hence, we have

$$F_z \approx t\int_S M_s\left(\frac{\partial}{\partial z}H^p_\perp + \frac{H^p_{||}}{H^t_\perp}\frac{\partial}{\partial z}H^p_{||}\right)dS. \quad (1)$$

The term $F_z^{(I)} = t\int_S M_s \frac{\partial}{\partial z}H^p_\perp dS$ describes the force on the probe due to a sample magnetized perpendicular to the film plane by $\mathbf{H}_0$ (see Fig. 1(a)). If M_s is uniform throughout the sample, this term will be zero, so only departures from uniformity will lead to a nonzero, spatially varying, contribution to the measured force which can be understood through theoretical calculations. The second term $F_z^{(II)} = t\int_S M_s(H^p_{||}/H^t_\perp)\frac{\partial}{\partial z}H^p_{||}dS$ in Eq. (1) describes the force on the probe due to the in-plane component of the sample magnetization induced by the magnetic field of the probe.

This expression for $F_z^{(II)}(z)$ can be used to extract values of M_s and $H^a_\perp$ from the experimentally measured dependence of the MFM force on z if the magnetic structure of the probe is well characterized and if the magnetic parameters of the sample can be considered constant over the effective probe-sample interaction range. Often it is possible to model the probe magnet as a point dipole of moment m_p; in this case, the z-dependence of $F_z^{(II)}$, evaluated by numerical integration, can be fit to the experimental data. Often the problem can be further simplified. The anisotropy field $H^a_\perp$ can be neglected when imaging a material with weak magnetic anisotropy such as permalloy. In addition, if $H_0 - 4\pi M_s \gg H^p_\perp$, then, we have

$$F_z^{(II)} \approx -\frac{3\pi}{2}\frac{M_s t}{H_0 - 4\pi M_s}\frac{m_p^2}{z^5}.$$

This expression, though applicable only in certain cases, offers a quick and easy way to evaluate M_s. It also provides an estimate of the spatial resolution achievable with this approach. This expression is derived under the assumption that M_s is constant throughout the region of strong probe-sample interaction: Eq. (1) leads to the result that this region is a circle of radius $R_i \approx 1.6z$.

We have applied this analysis to MFM data acquired while imaging an isolated (neighbors are 25 μm away), thin permalloy disk 5 μm in diameter and 40 nm thick. Fig. 2 shows spatial maps of a permalloy dot obtained at 4.2 K with the dot saturated in an out-of-plane magnetic field $H_0 = 12$ kG applied as shown in Fig. 1 using a cantilever with a Sm_2Co_{17} tip, resonant frequency 15.9 kHz, and spring constant ~ 0.25 N/m. Fig. 2 shows spatial maps acquired at several probe-sample separations. The static data, defined by the strength of the probe-sample force, are simpler to analyze than the dynamic, non-contact MFM data which are sensitive to factors such as energy dissipation in the probe-sample system. A detailed description of the experimental setup is available in Refs. 21 and 22.

The dependence of the static MFM force on separation was measured with the probe located directly over the center of the disk to guarantee that the region of the strong probe-sample interaction is entirely within the disk regardless of the magnitude of the separation. This is important because the analysis is derived for an infinite thin film and thus does not account for any possible edge-effects. In addition, with the probe centered over the disk, $F_z^{(I)}$ can be expressed analytically

$$F_z^{(I)} = -6\pi M_s d\frac{m_p z R^2}{(R^2+z^2)^{5/2}}, \quad (2)$$

where R is the radius of the dot.

Fig. 3 shows a numerical fit to the experimental data using Eq. (1) with M_s as a fitting parameter. In this case, $F_z^{(I)}$ was evaluated using Eq. (2) while $F_z^{(II)}$ was obtained by numerical integration because, in the case of Py, $H^p_\perp \sim 1$kG is comparable to $H_0 - 4\pi M_s \approx 2$ kG and, therefore, cannot be

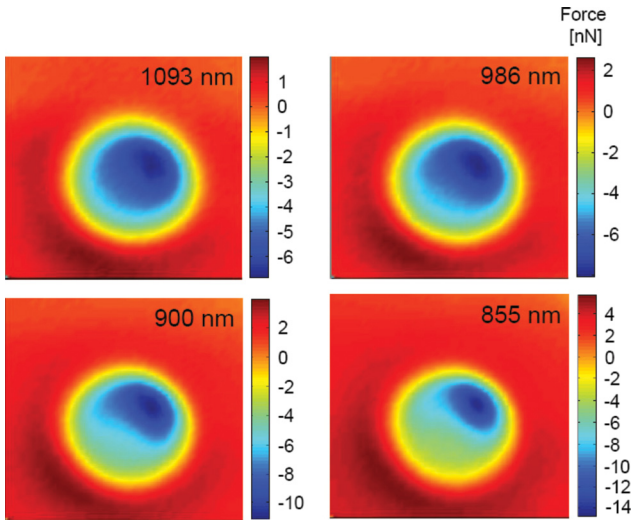

FIG. 2. (Color online) MFM images of the static cantilever deflection at several probe-sample distances $z = 1093$ nm, 986 nm, 900 nm, and 855 nm. z includes the effective tip radius $R_p \sim 500$ nm. The lateral size of the images is $10 \times 10\ \mu m^2$. We attribute the slight asymmetry in the images to the in-plane component of the probe's magnetic moment $\mathbf{m}_p$.

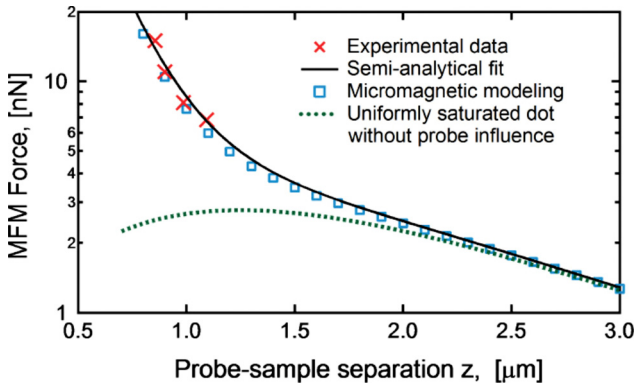

FIG. 3. (Color online) Dependence of the MFM force on separation z with the probe centered over the Py disk. Experimental data are obtained from MFM images in Fig. 2. The semi-analytical fit agrees excellently with experiment and returns $M_s \approx 803$ G. Micromagnetic modeling results for the same problem are shown for comparison. In addition, the separation dependence of the MFM force that would result if the disk was uniformly magnetized (obtained using Eq. (2)) is presented, clearly demonstrating the influence of the probe field on the magnetization structure of the dot.

neglected. The resulting value of $M_s \approx 803$ G is in excellent agreement with the generally accepted value of $M_s \approx 796$ G for permalloy.

Micromagnetic modeling confirms the validity of this analysis of the probe-sample interaction. The ground state magnetization of the disk was calculated in the presence of $\mathbf{H}_0$ and $\mathbf{H}_p$. As shown in Fig. 3, the numerically calculated MFM force agrees closely with both the experimental data and our simplified semi-analytical calculation.

The spatial resolution of the method is ultimately limited by the probe radius R_p which defines the minimum achievable radius of the probe-sample interaction region. Reducing the probe dimensions improves the spatial resolution at the expense of the probe magnetic moment m_p and hence the strength of the force signal. The current signal-to-noise ratio SNR $\sim 10^4$ allows a significant margin for probe miniaturization to dimensions as small ~ 100 nm, at which point the exchange interaction becomes significant and a more sophisticated analysis will be necessary.

In conclusion, we have demonstrated an imaging method for MFM characterization of thin magnetic films based on detecting the probe-induced magnetization of the sample. Local material parameters such as saturation magnetization and anisotropy field can be measured with excellent precision using this approach. We have presented an analysis of the MFM force response that is readily applicable for many cases; more complex situations can be analyzed by means of micromagnetic simulation.

This work was supported by the US Department of Energy through Grant No. DE-FG01-03ER46054 and by the NSF MRSEC program through Grant No. DMR-0820414.

[1]A. Hubert and R. Schafer, *Magnetic Domains: The Analysis of Magnetic Microstructures* (Springer, Berlin, 1998), pp. 78–85.
[2]J. J. Saenz, N. Garcia, P. Grutter, E. Meyer, H. Heinzelmann, R. Wiesendanger, L. Rosenthaler, H. R. Hidber, and H.-J. Guntherodt, J. Appl. Phys. **62**, 4293 (1987).
[3]M. Liebmann, A. Schwarz, U. Kaiser, R. Wiesendanger, D.-W. Kim, and T.-W. Noh, Phys. Rev. B **71**, 104431 (2005).
[4]T. Chang, J.-G. Zhu, and J. H. Judy, J. Appl. Phys. **73**, 6716 (1993).
[5]M. Koblischka and U. Hartmann, Ultramicroscopy **97**, 103 (2003).
[6]H. J. Hug, B. Stiefel, P. J. A. van Schendel, A. Moser, R. Hofer, S. Martin, H.-J. Guntherodt, S. Porthun, L. Abelmann, J. C. Lodder, G. Bochi, and R. C. OHandley, J. Appl. Phys. **83**, 5609 (1998).
[7]J. Lohau, A. Carl, S. Kirsch, and E. Wassermann, Appl. Phys. Lett. **78**, 2020 (2001).
[8]P. Kappenberger, I. Schmid, and H. J. Hug, Adv. Eng. Mater. **7**, 332 (2005).
[9]S. Schreiber, M. Savla, D. V. Pelekhov, D. F. Iscru, C. Selcu, P. C. Hammel, and G. Agarwal, Small **4**, 270 (2008).
[10]A. Wadas and H. J. Hug, J. Appl. Phys. **72**, 203 (1992).
[11]G. Matteucci, M. Muccini, and U. Hartmann, Phys. Rev. B **50**, 6823 (1994).
[12]J. Lohau, S. Kirsch, A. Carl, G. Dumpich, and E. F. Wassermann, J. Appl. Phys. **86**, 3410 (1999).
[13]T. Goddenhenrich, U. Hartmann, and C. Heiden, Ultramicroscopy **42–44**, 256 (1992).
[14]T. Ohkubo, J. Kishigami, K. Yanagisawa, and R. Kaneko, IEEE Trans. Magn. **29**, 4086 (1993).
[15]R. Proksch, E. Runge, P. K. Hansma, S. Foss, and B. Walsh, J. Appl. Phys. **78**, 3303 (1995).
[16]C. Israel, W. Wu, and A. de Lozanne, Appl. Phys. Lett. **89**, 032502 (2006).
[17]J. Vergara, P. Eamesa, C. Merton, V. Madurga, and E. D. Dahlberg, Appl. Phys. Lett. **84**, 1156 (2004).
[18]P. F. Hopkins, J. Moreland, S. S. Malhotra, and S. H. Liou, J. Appl. Phys. **79**, 6448 (1996).
[19]Z. Zhang and P. C. Hammel, Solid State Nucl. Magn. Reson. **11**, 65 (1999).
[20]B. C. Stipe, H. J. Mamin, T. D. Stowe, T. W. Kenny, and D. Rugar, Phys. Rev. Lett. **86**, 2874 (2001).
[21]T. Mewes, J. Kim, D. V. Pelekhov, G. N. Kakazei, P. E. Wigen, S. Batra, and P. C. Hammel, Phys. Rev. B **74**, 144424 (2006).
[22]Y. Obukhov, K. C. Fong, D. Daughton, and P. C. Hammel, J. Appl. Phys. **101**, 034315 (2007).